Joint Pathology Center
Veterinary Pathology Services

WEDNESDAY SLIDE CONFERENCE 2023-2024

Conference #5 — 20 September 2023

CASE I:

Signalment:
3-year-old, female spayed domestic short hair, feline (*Felis catus*)

History:
This patient had a history of unspecified respiratory problems and presented to the referring veterinarian in an agonal state. Prior to presentation, the cat developed sudden breathing difficulties followed by collapse.

Gross Pathology:
Gross examination reveals a carcass with a body condition score of 4 out of 5, mild dehydration and mild autolysis. The lungs have a moderate, diffuse, cobblestone appearance and are meaty with patchy red to dark red discoloration. On section, a small amount of mucoid, pale yellow material can be expressed from many bronchioles. There is a large amount of this material in the bronchi and distal two thirds of the trachea.

Microscopic Description:
Lung: The pulmonary architecture is disrupted by widespread fibrosis affecting the axial interstitium and many alveolar septa, creating pseudolobulation with frequent multifocal alveolar emphysema ('honeycombing'). Multiple alveolar septa are lined by pleomorphic, commonly low columnar epithelial cells with reactive nuclei (alveolar epithelial metaplasia) and there is type II pneumocyte hyperplasia. There are scattered foci of smooth muscle hyperplasia intermixed with the fibrous connective tissue. Variable cellular infiltrates, consisting mostly of neutrophils and macrophages, are present in alveoli rimming obliterated bronchioles. Bronchioles are filled with mucus and tend to be either denuded or lined by a mix of cuboidal and squamous epithelium.

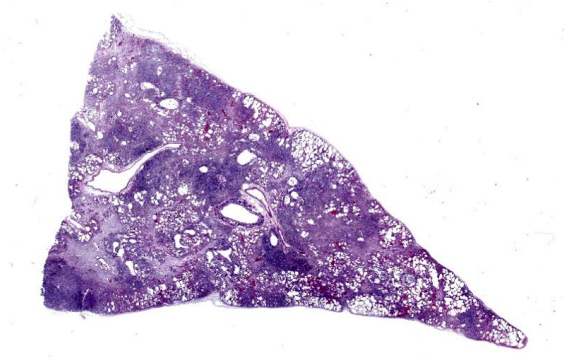

Figure 1-1. Lung, cat. In this section of lung, there is a nodularity to the parenchyma with areas of fibrosis and loss of architecture alternating with areas in which the alveolar septa are expanded and alveoli are variably ectatic ("honeycombing"). (HE, 6X)

Contributor's Morphologic Diagnosis:
Lung: Severe, chronic, bronchointerstitial pneumonia with marked alveolar septal and interstitial fibrosis, emphysema, alveolar epithelial columnar metaplasia, type II pneumocyte hyperplasia, and cuboidal to squamous metaplasia of bronchiolar epithelium.

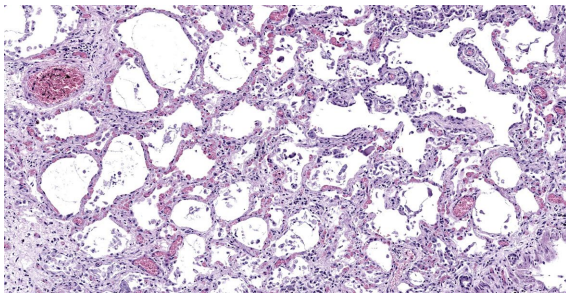

Figure 1-2. Lung, cat. Diffusely throughout the section, alveolar septa are expanded by collagen and fibroblasts, macrophages, and fewer neutrophils, and are often lined by type II pneumocytes. (HE, 121X)

Contributor's Comment:

The histologic appearance of the lung is consistent with feline idiopathic pulmonary fibrosis. Key histologic features of this uncommon condition as seen here include: 1) interstitial fibrosis with foci of fibroblast/myofibroblast proliferation, 2) columnar metaplasia of alveolar epithelium with type II pneumocyte hyperplasia (in some cases, mucous cell metaplasia is also common, but not seen in our case) and 3) smooth muscle hyperplasia/metaplasia.[1-3,5] This is similar to the histologic changes seen in idiopathic pulmonary fibrosis in humans.[5] This condition typically affects middle to older aged cats, although it has also been reported in cats under three years of age.[1-5] Presenting signs are largely respiratory related and include coughing, open mouth breathing, increased respiratory effort and rate, and respiratory distress.[1-5] Prognosis is usually poor and most individuals pass away within a year of presenting with respiratory signs despite treatment with steroids, bronchodilators, antibiotics and diuretics.[1-5] The cause for the condition is unknown, although a defect in type II pneumocyte development and function has been proposed.[1,5]

Contributing Institution:

Oregon State University
Corvallis, OR 97331
https://vetmed.oregonstate.edu/diagnostic

JPC Diagnosis:

Lung: Fibrosis, interstitial, diffuse, severe, with neutrophilic and histiocytic alveolitis, and smooth muscle and type II pneumocyte hyperplasia.

JPC Comment:

Feline idiopathic pulmonary fibrosis (FIPF) is one of several pulmonary diseases of veterinary importance that are characterized by fibrosis of the alveolar septa. Others include pulmonary fibrosis of West Highland Terriers, canine pulmonary fibrosis disease of unknown etiology, and equine multinodular pulmonary fibrosis, a helpfully named disease associated with equine herpesvirus-5.

As the contributor notes, the key histologic findings of FIPF include interstitial fibrosis with foci of fibroblasts or myofibroblasts, honeycombing of alveoli with alveolar epithelial metaplasia, and alveolar interstitial smooth muscle metaplasia.[1] These changes occur without a significant interstitial inflammatory infiltrate. The expansion of alveolar septa by fibrous connective tissue and smooth muscle leads to decreased pulmonary compliance, and the resulting pattern of respiratory distress is typically inspiratory or mixed inspiratory/expiratory. This distinguishes FIPF clinically from the more common bronchial-centered disorders in cats,

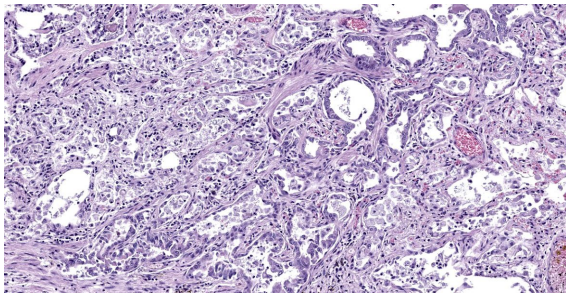

Figure 1-3. Lung, cat. Regionally, alveoli are lined by type II pneumocytes and contain large numbers of alveolar macrophages, fewer neutrophils, and cellular debris. (HE, 145X)

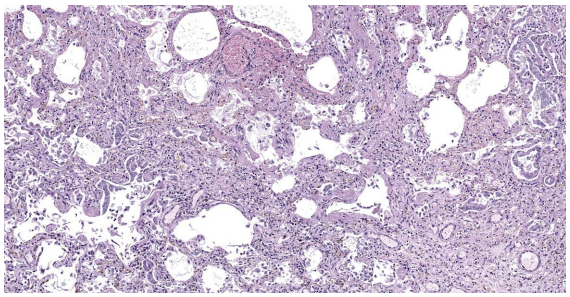

Figure 1-4. Lung, cat. Regionally, the fibrosis effaces alveolar architecture. (HE, 145X)

such as asthma and chronic bronchitis, which are characterized by expiratory distress.[1]

Definitive diagnosis of FIPF requires the demonstration of the previously described architectural and fibrous changes via histopathology. Published cases that include radiographic results report pronounced patchy to diffuse changes on thoracic radiographs, but the described changes are nonspecific and a mix of radiographic patterns has been described.[1-3] Bronchioalveolar lavage and fine needle aspirates can be used to rule out infectious causes for the clinical signs, but are unable to rule in a diagnosis of FIPF.[1]

While ante-mortem pulmonary biopsy can be useful for definitive diagnosis, care should be taken as up to 24% of cats in one study had concomitant pulmonary neoplasia, typically in areas of marked fibrosis.[1,4] This association is also seen in human cases of idiopathic pulmonary fibrosis, and when sampled as part of ante-mortem biopsy, pulmonary malignancy may complicate recognition of the concurrent FIPF which is often the primary cause of respiratory symptoms.[1,4]

Standard empiric therapies for feline respiratory disease, such as corticosteroids, rarely result in clinical improvement of FIPF patients, and a robust understanding of the disease pathogenesis is needed before therapeutic targets can be identified. Future treatments are likely to be focused on pharmacologic modulation of fibroblast-pulmonary parenchymal cell interactions, including TGF-β antagonists, inhibition of collagen-synthesis enzymes, and matrix metalloproteinase activity enhancement.[1]

This week's conference was moderated by MAJ Alicia Moreau, Chief of Education and Training and the Joint Pathology Center. MAJ Moreau discussed the terminology used to describe this condition in the veterinary literature. Of particular interest was the use of the term "alveolar epithelial metaplasia," which is often used as a key histologic feature of this entity. Participants felt this term was inconsistently or rarely defined in the literature, but in practice is often used to mean type II pneumocyte hyperplasia. Similar inconsistencies were noted with the term "honeycombing," which is defined differently depending on the source; however, most definitions contemplate confluent airspaces lined by cuboidal or hyperplastic epithelium and surrounded by fibrosis.

Conference participants felt that the defining histologic characteristic of this condition was the abundant fibrosis. Consequently, the JPC morphologic diagnosis leads with fibrosis while still acknowledging the mild inflammatory infiltrates present within the alveoli.

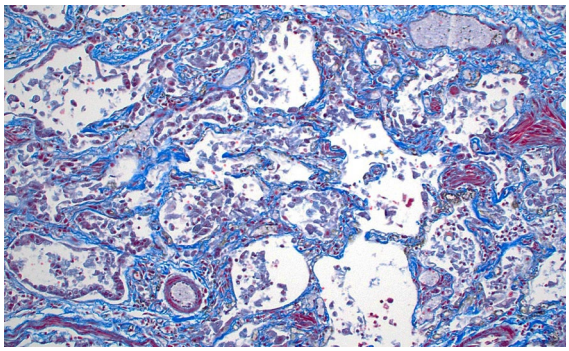

Figure 1-5. Lung, cat. A Masson's trichrome demonstrates the extent of the fibrosis in the section. (HE, 145X)

References:
1. Cohn LA, Norris CR, Hawkins EC, et al. Identification and characterization of an idiopathic pulmonary fibrosis-like condition in cats. *J Vet Intern Med*. 2004; 18(5):632-41.
2. Evola MG, Edmondson EF, Reichle JK, et al. Radiographic and histopathologic characteristics of pulmonary fibrosis in nine cats. *Vet Radiol Ultrasound*. 2014; 55(2):133-140.
3. Le Boedec K, Roady PJ, O'Brien RT. A case of atypical diffuse feline fibrotic lung disease. *J Feline Med Surg*. 2014; 16(10):858-863.
4. Reinero C. Interstitial lung diseases in dogs and cats part I: the idiopathic interstitial pneumonias. *Vet J*. 2019; 243: 48-54.
5. Williams K, Malarkey D, Cohn L, et al. Identification of spontaneous feline idiopathic pulmonary fibrosis: morphology and ultrastructural evidence for a type II pneumocyte defect. *Chest*. 2004; 125(6): 2278-2288.

CASE II:

Signalment:
4-year-old, male neutered Borzoi, canine (*Canis lupus familiaris*)

History:
The patient presented for unlocalized pain and frequent episodes of vocalization and was diagnosed with discospondylitis of the L3-L4 vertebrae. Surgical stabilization was performed and the dog was discharged with pain relief and empirical antibiotics. After initial improvement, the dog started to display pain and developed polyuria. Radiographs revealed a lytic lesion at the C4-C5 region. Azotemia with proteinuria developed, and cytological examination of the urine revealed numerous fungal hyphae. Culture of blood and urine was positive for *Rasamsonia (Geosmithia) argillacea*. Itraconazole therapy was implemented, but the patient declined rapidly and was euthanized.

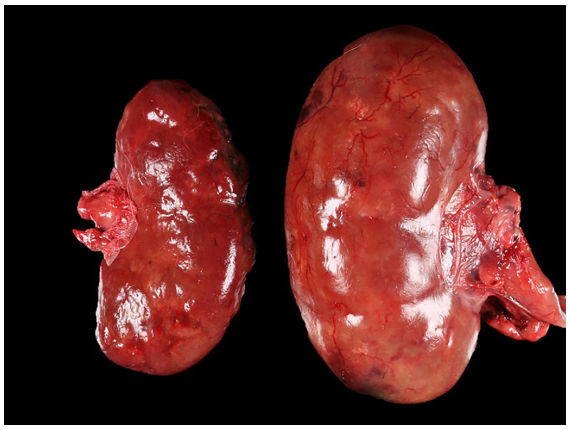

Figure 2-1. Kidney, dog. Enlargement of the right kidney with multifocal, 4-6 mm, white plaques on the cortical surface (fungal granulomas), and variably sized areas of hemorrhage. (Photo courtesy of: Massey University School of Veterinary Science, https://www.massey.ac.nz/about/colleges-schools-and-institutes/college-of-sciences/school-of-veterinary-science/)

Gross Pathology:
The patient was in a fresh state of preservation and poor body condition (BCS 2/9; total body weight 19kg), with generalised muscular atrophy and severe dehydration. Gross examination revealed enlargement of the right kidney with multifocal 4-6mm white plaques on the cortical surface interspersed with multifocal, variably sized areas of hemorrhage. There was severe bilateral pyelonephritis, with pyonephrosis of the right kidney. Multiple raised, pale, variably sized nodules were present in the splenic parenchyma and in two mesenteric lymph nodes. There was discospondylitis of the lumbar spine at the L3-L4 junction, and osteomyelitis of the cervical

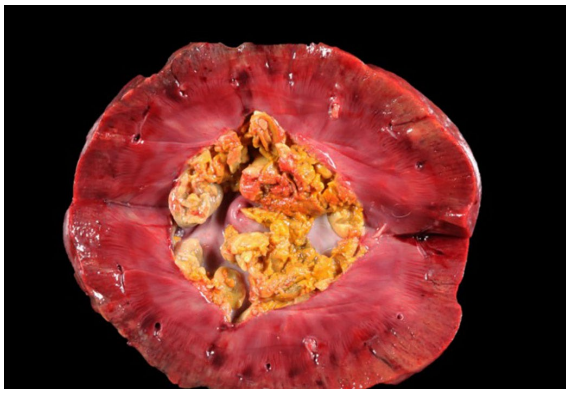

Figure 2-2. Kidney, dog. Severe bilateral pyelonephritis, with pyonephrosis of the right kidney. (Photo courtesy of: Massey University School of Veterinary Science)

spine at the C4-C5 region. The lungs appeared normal and no other abnormalities were noted.

Laboratory Results:
Rasamsonia (Geosmithia) argillacea was cultured from urine and blood.

Microscopic Description:
Kidney: Multifocally throughout the cortex, glomeruli and tubules are surrounded and replaced by numerous fibroblasts and abundant eosinophilic collagen bundles (interstitial fibrosis). Tubular epithelial changes include marked epithelial degeneration and necrosis characterized by swollen, vacuolated epithelial cells and shrunken hypereosinophilic, pyknotic cells, respectively. Deeply basophilic granular material (mineral), or bright eosinophilic homogenous material (protein) is present within the lumen of many tubules. Multifocally within the cortex are large aggregates of macrophages, lymphocytes, and plasma cells which surround large regions of amorphous eosinophilic material (fibrin), cellular debris, and 5-10µm diameter, fine, parallel walled, occasionally branching, septate hyphae and 5-7µm diameter conidia. These frequently appear adjacent to arcuate arteries and veins, with numerous PAS positive hyphae disrupting and invading the endothelium (angioinvasion) with marked endothelial necrosis characterized by shrunken, hypereosinophilic pyknotic cells, and destruction of the adventitia and tunica media. Within the renal pelvis, a large area of amphophilic necrotic debris is admixed with abundant PAS positive fungal hyphae and conidia. Multifocally throughout the cortex and medulla there are interstitial aggregates of lymphocytes and plasma cells.

Similar granulomatous inflammation, with PAS-positive fungal hyphae and conidia, is present within the mesenteric lymph nodes, spleen, and lumbar vertebral segment (not submitted).

Contributor's Morphologic Diagnoses:
1. Kidney: Nephritis, interstitial, granulomatous, chronic, multifocal, severe, with numerous PAS positive fungal hyphae and conidia, angioinvasion and marked interstitial fibrosis with cortical tubular degeneration and necrosis, acute, multifocal, marked.
2. Kidney: Pyelonephritis, chronic, granulomatous, with numerous PAS positive fungal hyphae and conidia.

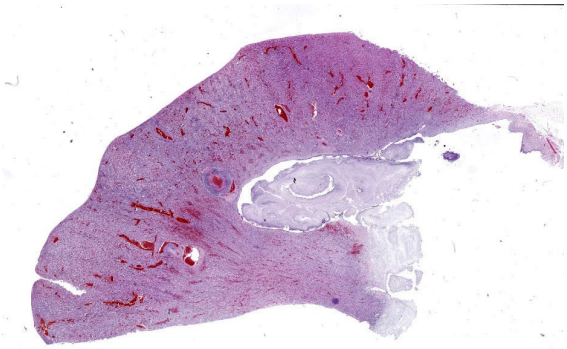

Figure 2-3. Kidney, dog. At subgross magnification, a large mat of fungus expands the renal pelvis, there are multiple chronic infarcts with flattening of the subcapsular surface, and cellular infiltrates around the arcuate arteries. (HE, 5X)

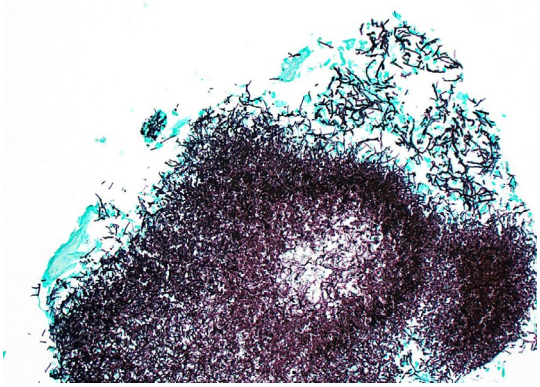

Figure 2-4. Kidney, dog. A GMS stain demonstrates a large mat of fungal hyphae within the renal pelvis. (GMS, 100X)

Contributor's Comment:

Here we present a case of disseminated systemic fungal infection with *Rasamsonia argillacea.* Fungal pyelonephritis with systemic dissemination is an uncommon clinical presentation in dogs, with the most common fungal isolate in canine pyelonephritis being *Aspergillus* spp., with *A. terreus* and *A. reflectus* the most frequently reported species.[2,4,8] *Cryptococcus* spp., *Candida* spp., *Penicillium* spp., *Paecilomyces* spp., *Sagenomella* spp., as well as systemic phaeohyphomycosis, are less commonly reported.[1,5]

In dogs, disseminated mycoses can clinically manifest as weight loss, lethargy, discospondylitis, osteomyelitis, urinary tract infections, polyuria, polydipsia, ophthalmitis, head tilt and gait difficulties.[4]

Rasamsonia is a recently described genus of saprobic thermotolerant fungal organisms of the Trichocomaceae family.[3] These are nonpigmented filamentous fungi and include four species that share phenotypic and genetic similarities: *R. argillacea, R. eburnean, R. piperina*, and *R. aegroticola.*[3] These fungi were previously classified as *Geosmithia* and *Talaromyces,* however recent studies reclassified the fungus as *Rasamsonia* based on genetic sequencing.[6,7]

The first case of disseminated *Rasamsonia* (referred to as *Geosmithia argillacea*) in humans or animals was reported in a German Shepherd.[5] German Shepherds appear overrepresented, perhaps owing to their susceptibility to disseminated fungal disease, particularly with *Aspergillus* spp.[2,9] IgA deficiency has been suggested as a possible predisposing factor for disseminated aspergillosis in this breed.[11,10] Other factors that may contribute to the German Shepherd's susceptibility to systemic fungal mycoses include depressed IgM responses or impaired mitogen-induced lymphocyte transformation.[11] In regard to *R. argillacea* infection, one study reported that five of eight dogs with *R. argillacea* were German Shepherds and six were spayed females.[3]

To our knowledge this is the first report of *Rasamsonia (Geosmithia) argillacea* causing disseminated disease in a dog in New Zealand or Australia. Due to the scant number of reported cases, the pathogenesis of *R. argillacea* infection is not well established. In most cases of systemic fungal mycoses, the portal of entry is usually unknown.[4] The most common portal of entry for fungal infections is the respiratory tract via inhalation, which then allows systemic spread after an initial respiratory infection.[4] Based on studies involving *Aspergillus* spp., the cycle begins with deposition of fungal conidia from the environment in the respiratory system.[4] Fungal species such as *Paecilomyces* spp. have also been reported to produce *in vivo* conidia, and these, along with the secondary spores produced, facilitate hematogenous spread.[4]

The portal of entry could not be identified in this case, which is consistent with the reported literature.[4] The presenting complaint

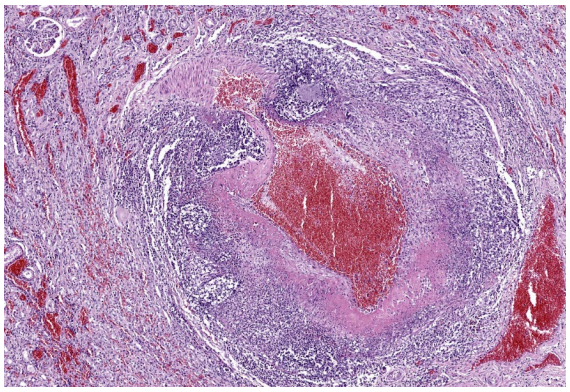

Figure 2-5. Kidney, dog. There is necrotizing arteritis of the arcuate arteries with extrusion of abundant pink proteinaceous material into the media and innumerable necrotic neutrophils in the media and adventitia. (HE, 62X)

of lumbar spinal pain with discospondylitis was the first indication of any clinical disease in this dog. The dog had a prior bout of suspected kennel cough, but this was over 12 months prior to the presentation of lumbar spinal pain, so perhaps this is where the initial infection was acquired. It is also possible that the infection was first acquired via the urinary tract, which then lead to pyelonephritis and systemic spread. Primary fungal pyelonephritis in dogs is only rarely reported.[5] In one case report, unilateral pyelonephritis was reported, with no evidence of systemic spread, indicating a possible ascending infection from the urinary tract.[5] In another case report, a primary fungal granuloma with *Paecilomyces variotii*, with no other evidence of systemic involvement was reported.[10] In both studies the primary route of entry could not be identified. It has also been suggested that immunosuppression due to other pathological conditions or immunosuppressive therapy may play a role.[4]

The gross and histological lesions in this case are astounding, with numerous fungal hyphae, granulomatous inflammation, angioinvasion and multinucleated giant cells within multiple organs. *Rasamsonia argillacea* appears to be an emerging pathogen in both human and animal medicine.[3] With the increasing reports in dogs, more research is needed to help further characterize *Rasamsonia* infections and to optimize diagnosis and treatment to improve overall prognosis.

Contributing Institution:
School of Veterinary Science
Massey University
Palmerston, North New Zealand 4442

JPC Diagnosis:
Kidney: Pyelonephritis, necrotizing and suppurative, focally extensive, severe, with fibrinous and necrotizing arteritis, multiple infarcts, and innumerable fungal hyphae.

JPC Comment:
The contributor provides an excellent overview of *Rasamsonia* infection in dogs. Though case reports are scarce, recent reports suggest that disseminated *Rasamsonia* infections commonly cause lesions in the spinal column, central nervous system, kidneys, spleen, lymph nodes, lungs, and heart.[3] *Rasamsonia* is considered an emerging pathogen, though it is frequently misidentified as *Penicillium* and *Paecilomyces* spp. based on morphologic similarities, and the apparent increase in incidence may be due, in part, to increased use of more accurate molecular speciation techniques in recent years.

This case is typical, in that the presenting complaint is often spinal pain due to *Rasamsonia* discospondylitis. Imaging studies of these patients typically reveal sclerotic and lytic vertebral lesions, most commonly in the thoracic spine.[3] These radiographic findings are similar to those in the relatively more common condition of disseminated aspergillosis, where approximately half of affected dogs show radiographic signs of discospondylitis.[9] Treatment in these cases is generally

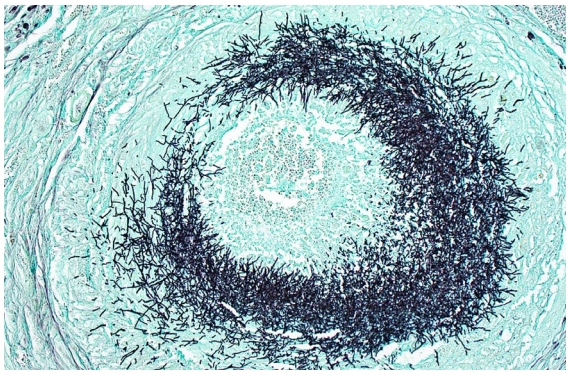

Figure 2-6. Kidney, dog. A GMS stain demonstrates numerous fungal hyphae in the necrotic arcuate arterial wall. (HE, 100X)

unsuccessful due to fungal resistance to available antifungal medications and the questionable ability of these medications to penetrate all affected tissues.[5]

In conference, discussion centered on the acute versus chronic nature of the observed histologic lesions. Large confluent areas of coagulative necrosis are present adjacent to the renal pelvis and in wedges extending from the medulla to the cortex. There are also extensive areas of fibrosis which represent more chronic insults arising from the damage to the arcuate arteries. Discussion also focused on the morphology of the dazzling fungal hyphae present in the renal pelvis and in arterial walls. Participants discussed differentials, including *Candida* spp. and *Penicillium* spp., and the need for fungal culture to identify the organism definitively.

References:

1. Day M, Holt P. Unilateral fungal pyelonephritis in a dog. *Vet Pathol*. 1994;31: 250-252.
2. Day M, Penhale W. An immunohistochemical study of canine disseminated aspergillosis. *Aus Vet J*. 1991;68:383-386.
3. Dear JD, Reagan KL, Hulsebosch SE, et al. Disseminated *Rasamsonia argillacea* species complex infections in 8 dogs. *J of Vet Int Med*. 2021;35:2232-2240.
4. Elad D. Disseminated canine mold infections. *Vet J*. 2019;243:82-90.
5. Grant DC, Sutton DA, Sandberg CA, et al. Disseminated *Geosmithia argillacea* infection in a German shepherd dog. *Med Mycol*. 2009;47:221-226.
6. Houbraken J, Giraud S, Meijer M, et al. Taxonomy and antifungal susceptibility of clinically important *Rasamsonia* species. *J of Clin Microbiol*. 2013;51:22-30.
7. Houbraken J, Spierenburg H, Frisvad JC. Rasamsonia, a new genus comprising thermotolerant and thermophilic *Talaromyces* and *Geosmithia* species. *Antonie Van Leeuwenhoek*. 2012;101:403-421.
8. Jang S, Dorr T, Biberstein E, Wong A. *Aspergillus deflectus* infection in four dogs. *J of Med and Vet Mycol*. 1986;24: 95-104.
9. Schultz RM, Johnson EG, Wisner ER, et al. Clinicopathologic and diagnostic imaging characteristics of systemic aspergillosis in 30 dogs. *J of Vet Int Med*. 2008;22:851-859.
10. Tappin S, Ferrandis I, Jakovljevic S, Villiers E, White R. Successful treatment of bilateral paecilomyces pyelonephritis in a German shepherd dog. *J of Small Ani Prac*. 2012;53:657-660.
11. Zhang S, Corapi W, Quist E, Griffin S, Zhang M. Aspergillus versicolor, a new causative agent of canine disseminated aspergillosis. *J of Clin Microbiol*. 2012;50: 187-191.

CASE III:

Signalment:

11-year-old, male intact common marmoset, primate (*Callithrix jacchus*)

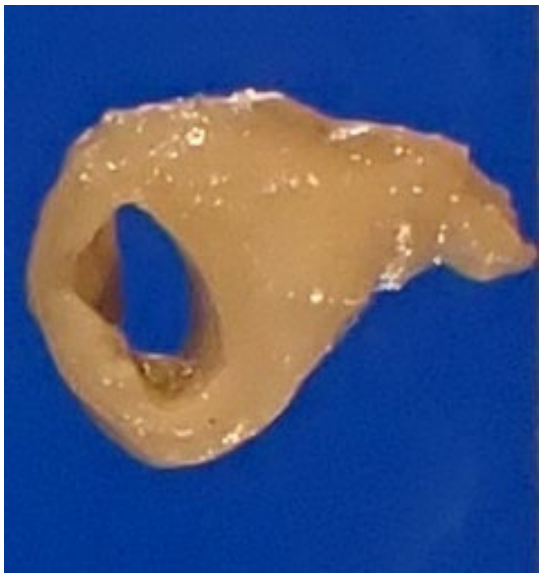

Figure 3-1. Duodenum, common marmoset. The small intestine from the level of the pylorus and extending distally 8cm was pale and thickened, measuring up to 7mm on cross section. (Photo courtesy of: Johns Hopkins University, Department of Molecular and Comparative Pathobiology, https://mcp.bs.jhmi.edu/)

History:
This male marmoset's clinical history included significant weight loss, poor body condition, chronic intermittent diarrhea, and progressive reticulocytosis, thrombocytosis, and hypoalbuminemia. Diagnostic evaluation ruled out infection by *Giardia* spp., *Klebsiella pneumoniae*, *Campylobacter coli*, *C. jejuni*, *Salmonella* spp., and *Shigella* spp., and revealed two biotypes of *E. coli* on fecal culture. Late in the disease course, there was radiographic evidence of an expansile lesion of the left patella. Treatment with nutritional support, antimicrobials, and immunomodulatory medications yielded minimal and transient improvement.

Gross Pathology:
Gross postmortem evaluation demonstrated little to no subcutaneous, visceral, or perirenal adipose tissue. Within all lung lobes were innumerable coalescing, firm, tan nodules, measuring up to 4 mm in diameter. The small intestine from the level of the pylorus and extending distally 8 cm was paler than the more normal, aborad, intestine. There was transmural thickening of the proximal duodenum, measuring up to 7 mm on cross section.

Laboratory Results:
Significant clinical pathology values: thrombocytosis (1,042 k/µL) and hypoalbuminemia (2.9 g/dL).

Microscopic Description:
Effacing and replacing approximately 75-80% of the pulmonary parenchyma are multiple neoplastic masses that are moderately well-demarcated, nonencapsulated, moderately cellular, and highly infiltrative. Neoplastic cells are arranged in a lepidic growth pattern along pre-existing alveolar septa and also form disorganized acini and clusters. Alveoli are expanded by lakes of mucin with paucicellular neoplastic cells aligned along remnant alveolar septa. Neoplastic cells are round to polygonal with variably distinct cell borders and frequently exhibit large intracytoplasmic clear vacuoles which marginate the nucleus (signet ring cells).

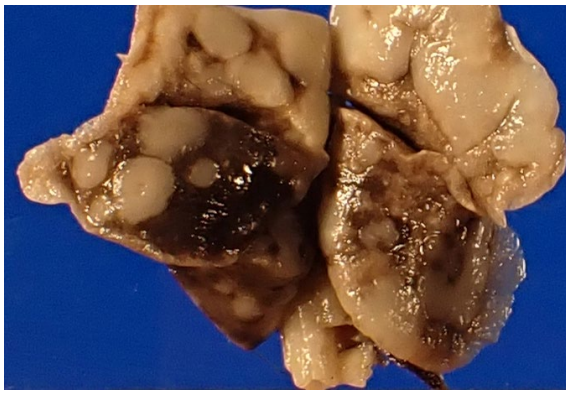

Figure 3-2. Lungs, common marmoset. Numerous nodules are present within all lung lobes, measuring up to 4mm. (Photo courtesy of: Johns Hopkins University, Department of Molecular and Comparative Pathobiology)

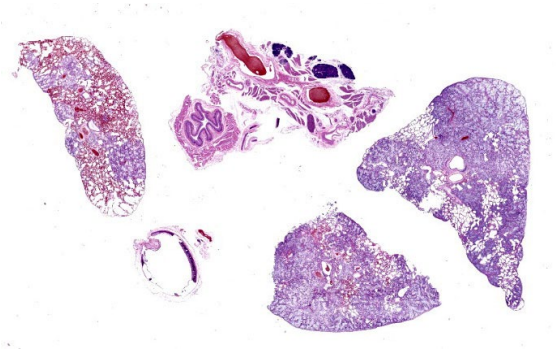

Figure 3-3. Lung, common marmoset. At subgross magnification, coalescing nodules of neoplasia are present within all cross-sections of lung. (Photo courtesy of: Johns Hopkins University, Department of Molecular and Comparative Pathobiology)(HE, 2x)

The nuclei contain one to three variably prominent eccentric nucleoli. The remainder of the cytoplasm is granular and moderately to deeply basophilic. Anisocytosis and anisokaryosis are moderate, and mitoses are rarely observed. Neoplastic cells are frequently clustered around medium sized vessels and expand and disrupt the tunica media and adventitia**.** There is moderate infiltration of neoplastic foci and alveoli with large foamy alveolar macrophages containing mucin and fewer lymphocytes. Alveoli frequently contain small amounts of eosinophilic proteinaceous fluid (edema) and fibrin. Alveolar septa are expanded in multiple areas by neoplastic cells, collagen fibers, edema, and inflammatory cells including lymphocytes and macrophages.

Contributor's Morphologic Diagnosis:
Lung: Metastatic duodenal mucinous adenocarcinoma.

Contributor's Comment:
This marmoset was euthanized following chronic clinical decompensation that was unresponsive to medical management. The clinical differential diagnoses in this case included Marmoset Wasting Syndrome (MWS), infectious enteropathies, and enteric neoplasia due to the thin body condition, diarrhea, bony lesions, and progressive hypoalbuminemia. Proximal duodenal mucinous adenocarcinoma with both local invasion and distant metastasis was diagnosed in this case, and wasting was attributable to chronic neoplastic and inflammatory changes of the intestine which likely impaired absorption and resulted in malnourishment.

Reports of small intestinal adenocarcinomas are uncommon in the gastrointestinal tract of aged nonhuman primates despite those of the large intestine being among the most frequently observed.[1,2,8,9] One limited case series and infrequent case reports have documented small intestinal adenocarcinomas in the marmoset.[1,3]

In marmosets, small intestinal adenocarcinomas typically begin as carcinomas *in situ* at the level of the jejunum or ileum before infiltrating the intestinal wall, and histology often demonstrates signet ring morphology and mucinous matrix.[3,4] Local invasion and metastasis to mesenteric lymph nodes were reported in 6/10 cases of marmoset small intestinal adenocarcinoma, but distant metastases were not noted.[3]

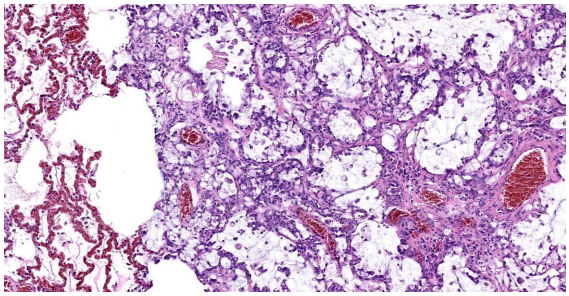

Figure 3-4. Lung, common marmoset. Neoplastic epithelial cells are present in nests and poorly formed glands and line alveolar septa. Alveolar lumina are often filled with mucin. (Photo courtesy of: Johns Hopkins University, Department of Molecular and Comparative Pathobiology) (HE, 131X)

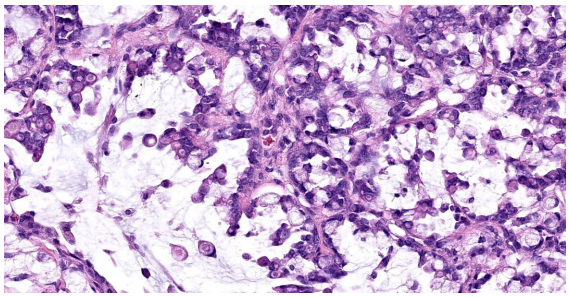

Figure 3-5. Lung, common marmoset. High magnification of neoplastic cells with abundant cytoplasmic mucus. (Photo courtesy of: Johns Hopkins University, Department of Molecular and Comparative Pathobiology) (HE, 131X)

The proximal duodenal localization in this case is atypical, as is the extensive metastatic disease. In this case, metastases were noted in the lungs, liver, and parapatellar adipose.[6] Additionally, the primary tumor and all metastases demonstrated absent to attenuated expression of pancytokeratin, indicating active neoplastic epithelial-mesenchymal transition and suggesting a poorer prognosis.[6] This case highlights the importance of considering infiltrative adenocarcinoma as a differential in captive marmosets exhibiting refractory weight loss and diarrhea.

Contributing Institution:
Johns Hopkins University
Department of Molecular and Comparative Pathobiology
Baltimore, MD 21230
https://mcp.bs.jhmi.edu/

JPC Diagnosis:
Lung: Mucinous adenocarcinoma, metastatic.

JPC Comment:
Adenocarcinomas arising in the small and large intestines of marmosets are rare and are thought to share a similar pathogenesis: dysregulation of the Wnt/ β-catenin signaling pathway.[4] This pathway is an evolutionarily conserved signaling cascade that regulates myriad cellular processes, including cell proliferation, differentiation, and apoptosis.[7] Under normal homeostatic conditions, β-catenin is subject to constitutive phosphorylation mediated by a complex of proteins, including the tumor suppressor gene product adenomatous poliposis coli (APC). The phosphorylation of β-catenin leads to its ubiquitination and subsequent proteosomal degradation, and prevents its accumulation in the cytosol.[7]

The activation of the canonical Wnt/ β-catenin pathway begins with the binding of the signaling ligand Wnt to Frizzled receptors at the plasma membrane. This binding recruits a variety of intracellular signaling proteins, including Disheveled and the APC complex, to the Frizzled receptor and inhibits the constitutive phosphorylation of β-catenin. Released from inhibition, β-catenin then accumulates in the cytosol, translocates to the nucleus, and activates Wnt-dependent gene expression.[7] In human colorectal cancers, this signaling sequence is most commonly perturbed by loss-of-function mutations in APC, leading to loss of β-catenin phosphorylation and degradation and, consequently, to unchecked cellular proliferation.

β-catenin also exerts influence outside of the Wnt signaling pathway through its interactions with cadherins, transmembrane proteins that mediate cell adhesion by linking the actin cytoskeletons of neighboring cells. β-catenin binds to the cytosolic domains of cadherins and stabilizes these normal cell to cell anchoring interactions. An increase in cytosolic β-catenin upsets this balance and can result in loss of cohesion among cells, a necessary precondition for metastasis.[4]

Though similar oncogenic mechanisms are at work throughout the intestinal tract, adenocarcinomas are far more likely to arise in the large intestine than in the small intestine.

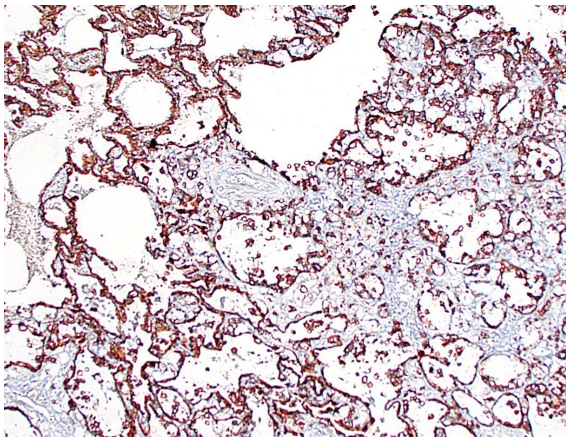

Figure 3-6. Lung, common marmoset. Neoplastic cells demonstrate strong cytoplasmic positivity for cytokeratin. (anti-AE1/AE3, 100X)

Factors currently thought to account for this disparity include: the faster transit time of digesta through the small intestine which decreases exposure to toxins when compared to the large intestine; the higher levels of IgA and mucosal-associated lymphoid tissue providing immune surveillance in the small intestine; and the increased distance between small intestinal crypt stem cells and the intestinal lumen which decreases exposure to luminal carcinogens.[4]

This case provoked a robust discussion among conference participants, several of whom felt they could not definitively rule out a primary pulmonary origin for this tumor. Immunohistochemical stains for TTF-1 and AE1/AE3 were examined during conference and largely served to confound. Though the contributor reported absent or attenuated pan-cytokeratin immunoreactivity, AE1/AE3 staining performed at the Joint Pathology Center revealed diffuse, strong cytoplasmic reactivity within the neoplastic cell population (Fig 3-6). The neoplastic cells were diffusely negative for TTF-1, a marker of primary pulmonary adenocarcinoma; however, there are case reports of TTF-1 negative primary pulmonary mucinous adenocarcinomas, including one recent case report in a marmoset.[5] Ultimately, the morphology of the tumor and the multifocal distribution in the lungs convinced participants that the tumor represented metastatic disease. Participants also briefly discussed the signet ring cells found through this section. Though interesting, signet ring cell morphology can also be found in melanomas and squamous cell carcinomas, among other tumors, and has no known prognostic significance.

References:

1. Brack M. Gastrointestinal tumors observed in nonhuman primates at the German primate center. *J Med Primatol*. 1998;27:319–324.
2. Johnson LD, Ausman LM, Sehgal PK, King NW. A prospective study of the epidemiology of colitis and colon cancer in cotton-top tamarins (Saguinus oedipus). *Gastroenterology*. 1996;110(1):102–115.
3. Miller AD, Kramer JA, Lin KC, Knight H, Martinot A, Mansfield KG. Small intestinal adenocarcinoma in common marmosets (Callithrix jacchus). *Vet Pathol*. 2010;47(5):969-976.
4. Miller AD. Chapter 18 - Neoplastic Diseases. In: Marini R, Wachtman L, Tardif S, Mansfield K, Fox J, eds. *The Common Marmoset in Captivity and Biomedical Research*. Academic Press 2019:305-309.
5. Mineshige T, Inoue T, Kawai K, et al. Spontaneous pulmonary adenocarcinoma in a common marmoset (*Callithrix jacchus*). *J Med Primatol.* 2021;50:335-338.
6. Peterson C, Plunkard J, Johanson A, Izzi J, Gabrielson K. Immunohistochemical characterization of a duodenal adenocarcinoma with pulmonary, hepatic and parapatellar metastases in a common marmoset (Callithrix jacchus). *J Comp Pathol*. 2021;189:1–7.

7. Silva-Garcia O, Valdez-Alarcón JJ, Baizabal-Aguirre VM. Wnt/β-catenin signaling as a molecular target by pathogenic bacteria. *Front. Immunol*. 2019;10:1-14.
8. Simmons HA, Mattison JA. The incidence of spontaneous neoplasia in two populations of captive rhesus macaques (Macaca mulatta). *Antioxid Redox Signal*. 2011;14(2):221–227.
9. Valverde CR, Tarara RP, Griffey SM, Roberts JA. Spontaneous intestinal adenocarcinoma in geriatric macaques (Macaca sp.). *Comp Med*. 2000;50(5): 540-544.

CASE IV:

Signalment:
12-day-old, Charolais bull, bovine (*Bos taurus*)

History:
The calf was unwell for 1 week and unable to suck with no response to antibiotic treatment. Only one calf was affected.

Gross Pathology:
The patient weighed 50 kg and was in age-appropriate body condition. Bilaterally the kidneys were tan-grey with an uneven subcapsular surface featuring multifocal pinpoint indentations. The calyces were oedematous.

Laboratory Results:
Urinalysis: Glucose = 14mml/l; Specific Gravity = 1.030; Protein = 2g/l; pH = 6; moderate number of nitrates; no leucocytes, urobilinogen, or RBCs.

Liver selenium: 71.50 umol/kg (normal range =5-20 umol/kg).

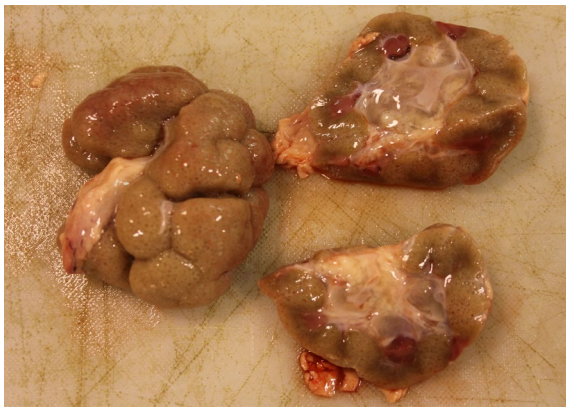

Figure 4-1. Kidney, calf. Bilaterally the kidneys were tan-grey with an uneven subcapsular surface featuring multifocal pinpoint indentations. The calyces were oedematous. (Photo courtesy of: Veterinary Sciences Centre, School of Veterinary Medicine, University College Dublin, Belfield, Dublin 4, Ireland, http://www.ucd.ie/vetmed/)

Zinc Sulphate Turbidity: Adequate colostral immunity.

Microscopic Description:
Kidney: The cortex is diffusely and markedly disrupted by large numbers of cystic spaces up to 120 um in diameter lined by a monolayer of cuboidal epithelium that is multifocally exfoliated and floating freely within these cystic lumens (autolysis). These cysts are separated by a large amount of fibro-myxoid, oedematous stroma that is composed of collagen bundles and plump fibroblasts. Multifocally, and predominantly within the cortex, are variably sized areas that exhibit pale eosinophilic, glassy, loose stroma with scattered stellate cells (primitive mesenchyme). Multifocally the glomeruli are small and mildly to moderately hypercellular with occasionally mildly thickened Bowman's capsules. Multifocally some glomeruli are irregularly lobulated. Multifocally the cortical tubules exhibit a small amount of luminal radiating achromatic crystalline material that is birefringent under polarized light (calcium oxalate crystals). Multifocally some of the cortical tubular epithelium exhibits a small

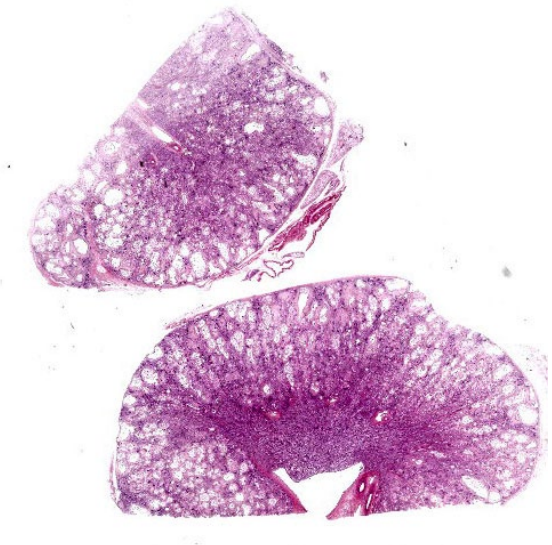

Figure 4-2. Kidney, calf. There is marked loss of tubules and remaining tubules are markedly ectatic. There are linear rays of fibrosis extending downward into the medulla which contain numerous fetal glomeruli and few sclerotic tubules. (HE, 27X)

amount of yellow, globular intracytoplasmic pigment. Multifocally medullary tubules exhibit dark basophilic epithelium that occasionally undergoes 'piling up.' Multifocally lumens within the medulla exhibit a small amount of eosinophilic, homogenous to glassy material (protein casts). Very rarely some of the tubules at the cortico-medullary junction exhibit ciliated epithelium (persistent mesonephric ducts). Multifocally interstitial blood vessels exhibit mildly thickened tunica media. Multifocally the stroma is infiltrated by small to moderate numbers of lymphocytes and plasma-cells (interstitial nephritis).

Contributor's Morphologic Diagnoses:

1. Kidney: Asynchronous maturation, interstitial fibrosis, with fetal glomeruli, immature tubules, primitive mesenchyme, persistent metanephric ducts, consistent with renal dysplasia.
2. Kidney: Lymphoplasmacytic nephritis, chronic, mild.

Contributor's Comment:

Renal dysplasia is defined as disorganised development of renal parenchyma due to anomalous differentiation and has been described in numerous species including humans, sheep, pigs, cats, horses and, most frequently, dogs.[2,11] The cause(s) of renal dysplasia are not well understood but are likely to be multifactorial and in some cases are considered congenital.[2] Proposed causes include genetic mechanisms, as well as in-utero infections and deficiencies affecting fetal development. Renal dysplasia has been identified in multiple dog breeds including the Golden Retriever, Beagle, Lhasa Apso, Great Dane, Dutch Kooiker dog, Samoyed, Alaskan Malamute, Cavalier King Charles Spaniel and Bulldog.[1,7,11,13] Renal dysplasia with hepatic fibrosis was described in Norwich terriers with INPP5E splice site variant causing lethal ciliopathy.[3] Examples of fetal infections resulting in renal dysplasia include panleukopenia virus in cats, canine herpes virus in dogs and BVDV infection in cattle.[10] In pigs, hypovitaminosis A is considered a cause of renal dysplasia.[2]

The gross presentation of the kidneys of affected animals varies, but affected kidneys are usually small, misshapen, fibrosed, and feature multiple cysts and tortuous ureters. One or both kidneys may be affected in an individual. In some cases, dysplastic kidneys show only minimal gross changes, such as having a slightly irregular contour.[2] The histopathological criteria to achieve a diagnosis of renal dysplasia include:

1. The presence of anomalous or undeveloped structures;
2. The presence of undifferentiated mesenchyme in the cortex or medulla;
3. Groups of immature glomeruli in non-neonatal animals;

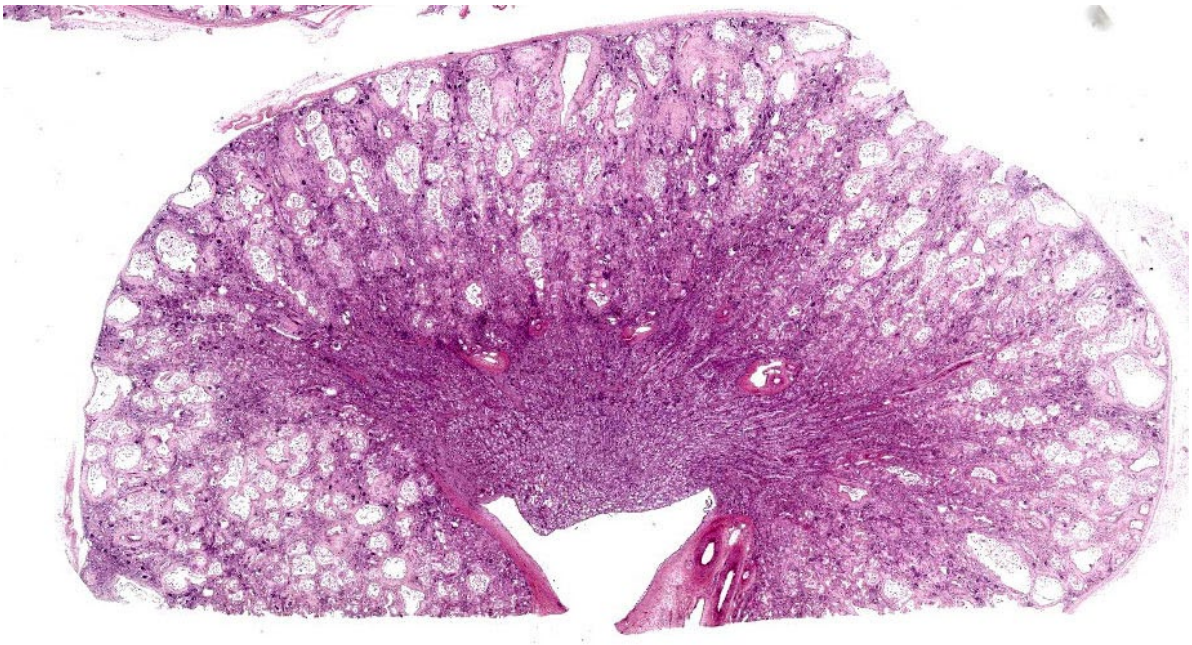

Figure 4-3. Kidney, calf: Normal cortical architecture is replaced by large ectatic tubules separated by areas of fibrosis and fetal glomeruli. The change is largely restricted to the cortex. (HE, 87)

4. Lack of glomeruli or tubules in some lobes of the kidneys;
5. Collecting tubules with blind ends within cortical connective tissue;
6. Atypical tubular epithelium;
7. The presence of primitive (metanephric) ducts lined by cuboidal or columnar epithelium; and
8. Dysontogenic (cartilaginous or osseous) metaplasia, mainly seen in humans.[2]

Because ureteral anomalies are often present in cases of renal dysplasia, dysplastic kidneys are also highly susceptible to developing pyelonephritis. Various forms of renal dysplasia and nephropathy have been described in ruminants, including: renal dysplasia in Japanese black cattle;[12] autosomal dominant cystic renal dysplasia in Suffolk sheep;[8] renal dysplasia with hydronephrosis and congenital ureteral strictures of unknown cause in two Holstein-Friesian calves;[15] immune mediated mesangiocapillary glomerulonephritis in Finnish Landrace lambs (cause unknown but thought to represent a recessive, inherited defect of the complement system);[5] nephropathy in Japanese black cattle caused by a claudin 16 gene deletion mutation;[6] and familial glomerulopathy and peripheral neuropathy in Gelbvieh cattle.[9]

The cause of the renal dysplasia in the case presented here remains unknown. Both calf and dam were negative for BVDV and no abnormalities were found in other tissues. The significance of the very high liver selenium concentration remains unclear.

Contributing Institution:
Veterinary Sciences Centre
School of Veterinary Medicine
University College Dublin
Belfield, Dublin 4, Ireland
http://www.ucd.ie/vetmed/

JPC Diagnosis:
Kidney: Asynchronous maturation with fetal glomeruli, tubular loss, marked interstitial fibrosis, and mild lymphoplasmacytic interstitial nephritis.

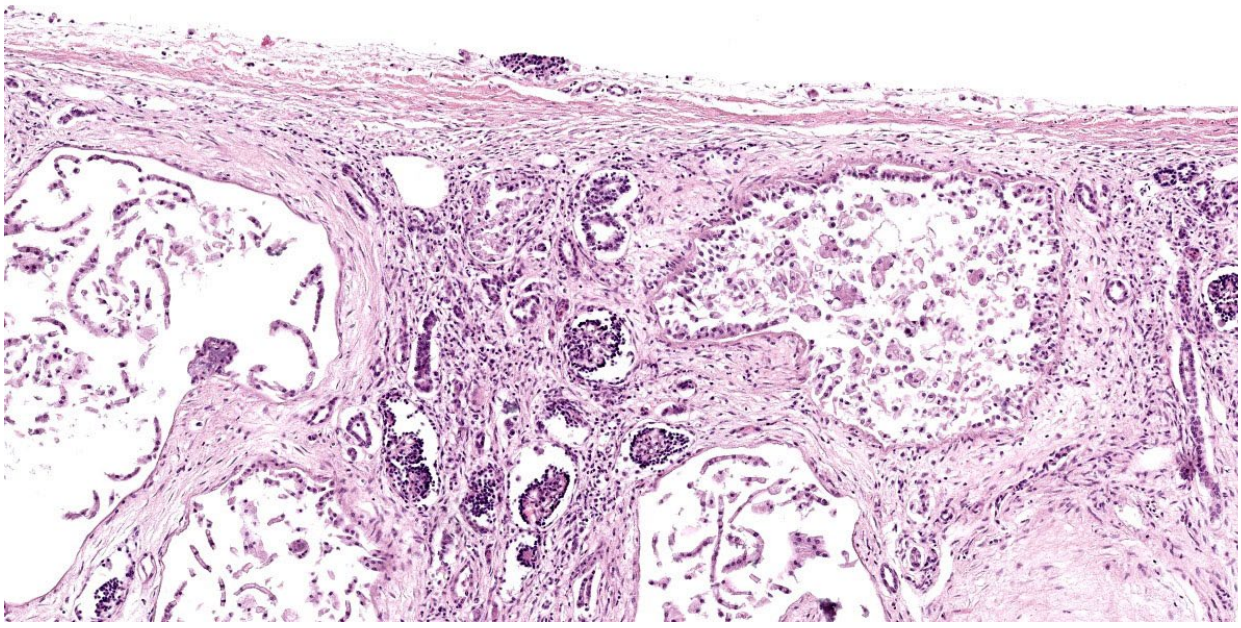

Figure 4-4. Kidney, calf. Segmentally in the cortex, there are rays of fibrous connective tissue extending to the capsule which contain numerous fetal glomeruli and atrophic tubules. (HE, 87)

JPC Comment:
Renal dysplasia is a broad term that encompasses a range of gross and histologic abnormalities caused by development gone rogue. In mammals, two precursor kidneys are formed prior to the arrival, in the mature animal, of the metanephric kidney. The first is the pronephros, which contains primitive tubules and a pronephric duct, that grows caudally and terminates in the fetal cloaca.[4] The tubules of the pronephros degenerate, but the pronephric duct persists as the mesonephric duct. The mesonephric duct, in turn, induces the formation of the mesonephric kidney, which consists of tubules that terminate in vascular proliferations arising from the dorsal aorta on one end and the mesonephric duct on the other. In amphibians and fish, the mesonephros becomes the functional mature kidney. In reptiles, birds, and mammals, the mesonephros degenerates, setting the stage for the arrival of the metanephros.[4]

The metanephric kidney beings as an evagination from the mesonephric duct, called the ureteric bud.[11] The ureteric bud moves cranially and differentiates into the ureter, renal pelvis, and collecting ducts. The ureteric bud grows into a mass of mesenchymal cells known as the metanephrogenic mass or the metanephric blastema. As the ureteric bud successively divides into collecting ducts, these ducts induce nephrogenic differentiation of the metanephric blastema. These proto-nephrons elongate, canalize and induce the formation of immature glomeruli at one end, and connect with the collecting ducts at the other. Nephrons continue to develop from deep to superficial within the kidney and, in some species, continue to form and mature after birth.

The term renal dysplasia implies disorder of the complex interactions between the ureteric bud and the metanephric blastema, resulting in anomalous metanephric differentiation.[11] The contributor outlines several canonical histologic criteria, at least one of which must be present for a diagnosis of renal dysplasia. Two of these criteria, the presence of metanephric ducts surrounded by primitive mesenchyme and the formation of dysontogenic tissues, both indicate total failure of the initial

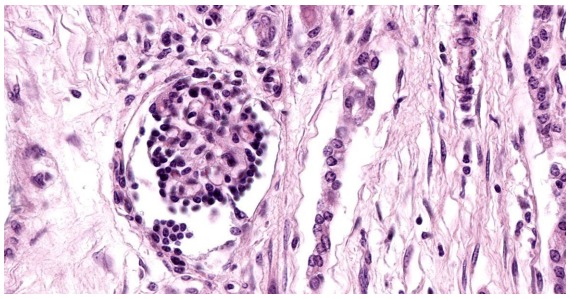

Figure 4-5. Kidney, calf. Fetal glomerulus. (HE, 400X)

interaction between the ureteric bud and the metanephric blastema.[11] In contrast, the presence of fetal glomeruli and tubules, the presence of persistent mesenchyme, and the presence of anomalous structures indicate that the induction of the metanephric blastema was initiated but failed to undergo complete differentiation.[11]

As the contributor notes, ureteral anomalies are common in cases of renal dysplasia. This is unsurprising given the close developmental relationship between the kidney and the collecting system. Among the reported ureteral anomalies associated with renal dysplasia are ectopic ureters, ureteral obstruction with accompanying hydronephrosis, hydroureter, and congenital urothelial cell hyperplasia.[10,14,15]

Conference discussion focused on the difficulty of definitively identifying structures, such as persistent metanephric ducts or primitive mesenchyme, amid the histologic noise present in a kidney as dysplastic as the section examined in conference. While fetal glomeruli are more obvious, their presence can be a normal finding in the neonates of some species, such as dogs, in which renal development continues through the first few weeks of life.

Discussion also focused on the term "renal dysplasia," which has fallen somewhat out of favor due to its relatively elastic meaning which has become somewhat overstretched over time due to inconsistent use. The currently proposed term, "renal maldevelopment," is meant to describe the disorganized development of renal parenchyma exemplified by this case. The term "renal dysplasia," while well-ensconced in the veterinary literature, should be thought of as an umbrella term, covering a heterogenous group of renal developmental anomalies.

References:

1. Bruder MC, Shoieb AM, Shirai N, Boucher GG, Brodie TA. Renal dysplasia in Beagle dogs: four cases. *Toxicol Pathol*. 2010;38(7):1051-1057.
2. Cianciolo RE, Mohr FC. Urinary system. In: Maxie MG, ed. *Jubb, Kennedy,and Palmer's Pathology of Domestic Animals*. Vol. 2. 6th ed. Philadelphia, PA: Elsevier; 2016:393.
3. Dillard KJ, Hytönen MK, Fischer D, et al. A splice site variant in INPP5E causes diffuse cystic renal dysplasia and hepatic fibrosis in dogs. *PLoS One*. 2018;13(9):e0204073.
4. Fletcher TF, Weber AF. Veterinary developmental anatomy (veterinary embryology). University of Minnesota College of Veterinary Medicine. 2013. Accessed September 20, 2023. http://vanat.cvm.umn.edu/vanatpdf/EmbryoLectNotes.pdf.
5. Frelier PF, Armstrong DL, Pritchard. Ovine mesangiocapillary glomerulonephritis type I and crescent formation. *Vet. Pathol.* 1990;27(1):26-34.
6. Hirayama H, Kegeyama S, Moriyasu S, et al. Genetic diagnosis of claudin 16 deficiency and sex determination in bovine preimplantation embryos. *J. Reprod. Dev.* 2004; 50:613-618.
7. Kerlin R., Van Winkle TJ. Renal dysplasia in Golden Retrievers. *Vet. Pathol.* 1992; 32:327-329.

8. O'Toole D, Jeffrey M, Jones T, Morgan G, Green R. Pathology of renal dysplasia and bladder aplasia-hypoplasia in a flock of sheep. *J. Vet. Diagn. Invest.* 1993; 5:591-602.
9. Panciera RJ, Washburn KE, Streeter RN, Kirkpatrick JG. A familial peripheral neuropathy and glomerulopathy in Gelbvieh calves. *Vet. Pathol.* 2003;40 (1):63-70.
10. Percy DH, Carmichael LE, Albert DM, King JM, Jonas AM. Lesions in puppies surviving infection with canine herpesvirus. *Vet Pathol.* 1971;8(1):37-53.
11. Picut CA, Lewis RM. Microscopic features of canine renal dysplasia. *Vet Pathol.* 1987;24(2):156-163.
12. Sugiyama A, Ozaki K, Miyazaki, Tanabe Y, Takeuchi T, Narama I. Renal dysplasia unrelated to claudin-16 deficiency in Japanese Black cattle. *J Comp Pathol.* 2007;137(1):71-77.
13. Whiteley MH, Bell JS, Rothman DA. Novel allelic variants in the canine cyclooxgenase-2 (Cox-2) promoter are associated with renal dysplasia in dogs. *PLoS One*. 2011;8;6(2):e16684.
14. Yoon HY, Mann FA, Punke JP, Jeong SW. Bilateral ureteral ectopia with renal dysplasia and urolithiasis in a dog. *J Am Anim Hosp Assoc*. 2010;46(3):209-214.
15. Yoshida K, Takezawa S, Itoh M, Takahashi E, Inokuma H, Watanabe K, et al. Renal dysplasia with hydronephrosis and congenital ureteral stricture in two Holstein-Friesian calves. *J Comp Pathol.* 2022;193:20-24.